# Putamen–midbrain functional connectivity is related to striatal dopamine transporter availability in patients with Lewy body diseases

NeuroImage: Clinical 8 (2015) 554–559

Contents lists available at ScienceDirect

NeuroImage: Clinical

journal homepage: www.elsevier.com/locate/ynicl

# Putamen–midbrain functional connectivity is related to striatal dopamine transporter availability in patients with Lewy body diseases

A. Rieckmann[a,b], S.N. Gomperts[c,d], K.A. Johnson[d,e], J.H. Growdon[d], K.R.A. Van Dijk[a,f,*]

[a]Department of Radiology, Athinoula A. Martinos Center for Biomedical Imaging, Massachusetts General Hospital, Charlestown, MA 02129, USA
[b]Department of Radiation Sciences, Diagnostic Radiology, Umeå University, Umeå, Sweden
[c]MassGeneral Institute for Neurodegenerative Disease, Boston MA 02129, USA
[d]Department of Neurology, Massachusetts General Hospital, Boston, MA 02114, USA
[e]Division of Nuclear Medicine and Molecular Imaging, Massachusetts General Hospital, Boston, MA 02114, USA
[f]Harvard University, Department of Psychology, Center for Brain Science, Cambridge, MA 02138, USA

ARTICLE INFO

*Article history:*
Received 12 March 2015
Received in revised form 1 June 2015
Accepted 2 June 2015
Available online 9 June 2015

*Keywords:*
Functional connectivity
fMRI
PET
Dopamine transporter
Lewy body diseases

ABSTRACT

Prior work has shown that functional connectivity between the midbrain and putamen is altered in patients with impairments in the dopamine system. This study examines whether individual differences in midbrain–striatal connectivity are proportional to the integrity of the dopamine system in patients with nigrostriatal dopamine loss (Parkinson's disease and dementia with Lewy bodies). We assessed functional connectivity of the putamen during resting state fMRI and dopamine transporter (DAT) availability in the striatum using 11C-Altropane PET in twenty patients. In line with the hypothesis that functional connectivity between the midbrain and the putamen reflects the integrity of the dopaminergic neurotransmitter system, putamen–midbrain functional connectivity was significantly correlated with striatal DAT availability even after stringent control for effects of head motion. DAT availability did not relate to functional connectivity between the caudate and thalamus/prefrontal areas. As such, resting state functional connectivity in the midbrain–striatal pathway may provide a useful indicator of underlying pathology in patients with nigrostriatal dopamine loss.



## 1. Introduction

Dopamine cells of the midbrain (substantia nigra and ventral tegmental area) heavily innervate the striatum. Loss of dopaminergic cells in the midbrain is a neuropathological hallmark of age-related Lewy body diseases (LBD) including Parkinson's disease with or without dementia and dementia with Lewy bodies. Nigrostriatal dopamine loss can currently only be measured in vivo using positron emission tomography (PET). Striatal dopamine transporter (DAT) availability measured with PET is one measure of nigrostriatal integrity (see Brooks and Pavese, 2011, for review). DAT binding in putamen and caudate in patients with LBD is reduced by 55–75% compared to age-matched controls (Innis et al., 1993; O'Brien et al., 2004) and correlates with nigrostriatal neuron loss observed post-mortem (Colloby et al., 2012).

Consistent with known projections, the striatum and midbrain are functionally coupled as measured with functional magnetic resonance imaging (fMRI) during resting state in healthy adults (Kelly et al., 2009; Hacker et al., 2012). Studies in patients with Parkinson's disease have shown that midbrain–putamen functional connectivity is reduced compared to age-matched healthy controls (Hacker et al., 2012; Wu et al., 2012), suggesting that loss of striatal resting-state functional connectivity may be reflective of the nigrostriatal dopamine loss in these patients. In line with this hypothesis, Tomasi and Volkow (2014) showed increases in midbrain coupling with ventral striatum and pallidum in children with attention deficit hyperactivity disorder (ADHD), which may parallel the increased levels of markers of the dopamine system that are seen in ADHD (e.g. Spencer et al., 2013). In schizophrenic patients, midbrain connectivity with ventral striatum was decreased (Hadley et al., 2014), again possibly reflecting altered functions of the dopamine system in this patient group (Laruelle et al., 1996).

To date, however, reports have been restricted to group comparisons between patient groups with known pathology of the dopamine system, without an analysis of individual differences in midbrain–striatal connectivity in relation to in vivo assessments of dopamine PET markers. The present study was designed to fill this gap by assessing striatal connectivity with resting-state fMRI and DAT availability with PET in the same group of patients with nigrostriatal dopamine loss. We predicted that weaker functional connectivity MRI between the midbrain and the putamen would be related to lower presynaptic DAT availability in the striatum. If present, such a result would indicate

*Abbreviation list:* LBD, Lewy body diseases; DAT, dopamine transporter; UPDRS, Unified Parkinson's Disease Rating Scale; ROI, region of interest; DVR, distribution volume ratio.

* Corresponding author at: Department of Radiology, Athinoula A. Martinos Center for Biomedical Imaging, 149 13th Street, Charlestown, MA 02129, USA.
*E-mail address:* kvandijk@nmr.mgh.harvard.edu (K.R.A. Van Dijk).

http://dx.doi.org/10.1016/j.nicl.2015.06.001

that resting-state functional connectivity MRI may function as a useful biomarker of underlying neuropathology.

## 2. Materials and methods

### 2.1. Participants

Twenty-six patients (mean age = 68.1 years, SD = 6.7, range 57–81, 9 female) with parkinsonism completed a PET scan, a structural MRI and at least one resting-state fMRI run. Data from six of these patients were excluded from analysis because of head motion (Van Dijk et al., 2012).

Subjects were recruited from the MGH Movement Disorders and Memory Disorders Units. All subjects gave informed consent to participate in the study according to the protocol approved by the ethical review board. Patients were clinically diagnosed with parkinsonism and had, on average, experienced motor symptoms for 9.2 years (SD = 5.6, range 3–22 years). Fourteen patients met diagnostic criteria for idiopathic Parkinson's disease (Hughes et al., 1992) and were non-demented. Six other patients were diagnosed with parkinsonism and cognitive impairment: three had dementia with Lewy bodies (McKeith et al., 2005) and three had Parkinson's disease with dementia (Emre et al., 2007). Although it is worthwhile to study these patient groups separately when large sample sizes permit (e.g. Marquie et al., 2014), in the current study the primary objective was to study striatal functional connectivity in relation to dopamine loss as measured with PET. As all subjects shared the typical motor signs of parkinsonism, and as DAT density was depleted in all patients relative to a healthy reference sample, patients were treated as a single group.

Patients were tested on their prescribed dopamine replacement medication to minimize head motion and a levodopa equivalent dose was calculated (mean = 400.3 mg/day, SD = 376.8; Tomlinson et al., 2010). Motor impairment was classified according to Hoehn and Yahr criteria (mean = 2.5, SD = 0.6, range 2–4) and the Unified Parkinson's Disease Rating Scale motor subscale (UPDRS; mean = 20.7, SD = 8.4, range 8–37; data missing for one individual).

Data from twenty-nine clinically normal older adults were used as reference sample to (1) demonstrate that our PET measure accurately separates DAT densities in clinically normal aging from pathological dopamine loss and (2) to identify reference seeds for the functional connectivity analyses. Control subjects were clinically normal older adults (mean = 70.9 years, range 63–80, 11 females) recruited for the Harvard Aging Brain study. Patients and normal controls did not differ in terms of age ($t(47) = 1.0$, $p = 0.34$) or estimated VIQ (mean(±SD) patients = 122.5(11.4), mean(±SD) controls = 120.9(9.6); $t(46) = -0.5$, $p = 0.62$; based on the American National Reading Test; Ryan and Paolo, 1992). Healthy controls were slightly lower in years of education (mean(±SD) patients = 16.2(3.2), mean(±SD) controls = 14.4(2.8); $t(47) = -2.1$, $p = 0.04$). Data from these patients and normal control participants have been presented elsewhere (Marquie et al., 2014; Schultz et al., 2014; Shaw et al., 2015).

### 2.2. PET acquisition and analysis

Binding of 11C-Altropane, a ligand with high selectivity for striatal DAT (Fischman et al., 2001), was assessed with an HR+ (CTI, Knoxville, TN) PET camera (3D mode, 63 adjacent slices of 2.42 mm interval, 15.2 cm axial field of view, 5.60 mm transaxial resolution). Approximately 15 mCi of 11C-Altropane was intravenously administered as a bolus over 20–30 s. Dynamic images were acquired in 39 frames of increasing duration for a total of 60 min ($8 \times 5$ s, $4 \times 1$ min, $27 \times 2$ min). PET data were reconstructed using a filtered back-projection algorithm and standard photon attenuation measurements were used to correct the emission data. The participant's head was stabilized during the scan and correction for residual head motion was performed on the dynamic data to a common reference frame.

PET data were partial volume corrected using an anatomical MRI-based correction method, implemented using PVElab Software and SPM5 (Quarantelli et al., 2004; Meltzer et al., 1990). Then, uptake images (averaged across the first 8 min) were normalized to the SPM8 standard PET template in MNI space using a two-step procedure of an initial 12-parameter affine transformation followed by non-linear warping (http://www.fil.ion.ucl.ac.uk/spm). Normalization parameters were applied to the remaining frames and a striatum region of interest (ROI) was defined as the 1000 voxels (=8 $cm^3$) with the highest signal intensity on the average emission image (8–60 min, Fig. 1A). The search was constrained to a large search area around the striatum. A central cerebellar region of 1000 voxels was defined in MNI atlas space as a reference region and Logan graphical analysis was used to derive distribution volume ratios (DVRs; Logan et al., 1990) for the striatum. Alternative methods for PET ROI delineation of striatum involve manual or automatic delineation in native PET or MRI space. However, anatomical ROI estimates can be inaccurate due to low spatial resolution or low contrast and also differ in size between individuals, which may introduce dependencies between volume measures and DVR. Our approach ensured that DVR estimation for the striatum is fully automated, of a fixed size, and not affected by moderate errors in the registration to standard space. Even though this approach does not distinguish between sub-regions of the striatum it accurately separates DAT densities in clinically normal aging (mean = 3.38, SD = 0.34) from pathological dopamine loss in the patients (mean = 2.02, SD = 0.29; $t(47) = 14.70$, $p < 0.01$; Fig. 1B) and the DVR estimates correlated significantly with disease duration ($r = -0.45$, $p = 0.02$) and Hoehn–Yahr stage of motor impairment ($r = -0.45$, $p = 0.03$) in the present sample.

### 2.3. MRI acquisition and analysis

All patients completed a T1-weighted MPRAGE scan (1.0 mm isotropic voxel size, TR = 2300 ms, TE = 2.98 ms, Flip angle 9 deg, 192 slices) and at least one resting state fMRI run of 6 min and 30 s using a T2*-weighted sequence sensitive to blood oxygenation level dependent contrast (2.0 mm isotropic voxel size; TR = 5000 m, TE = 30 ms, flip angle 90 deg, 55 slices). For normal controls, a multiecho MPRAGE (1.20 mm isotropic voxel size, TR = 2200 ms, TI = 1100 ms, Flip angle = 7 deg, 4× acceleration, 144 slices, TE = 1.54, 3.36, 5.18, 7.01 ms) and two resting state fMRI runs of 6 min and 20 s were available (3.0 mm isotropic voxel size, TR = 3000 ms, TE = 30 ms, Flip angle = 85 deg, 47 slices). All MRI scans were acquired on a Siemens 3 T Tim Trio scanner at Massachusetts General Hospital.

From the T1-weighted structural scan, ventricular size was estimated from a volumetric segmentation using Freesurfer (v 5.1.0, e.g. Fischl et al., 2002). Ventricle volume was normalized by intracranial volume following the methods described in Buckner et al. (2004), and used to control for the effects of subcortical atrophy in the association between functional connectivity and striatal DVR.

Pre-processing of the fMRI data followed the procedures of prior studies in this field (di Martino et al., 2008; Hacker et al., 2012) and included slice-timing correction, motion-correction, registration to standard MNI152 space, spatial smoothing, temporal filtering, and intensity normalization. Motion-correction was performed using rigid body translation and rotation of all volumes to the first volume (Jenkinson et al., 2002). To acquire a summary measure of motion, the root-mean-square of the 3 translation and 3 rotation parameters was calculated for each volume relative to the preceding volume and averaged over all volumes of the scan. Following this step, six patients were excluded from further analysis (N = 20 remaining) because they had an average mean displacement of more than 0.25 mm, where 0.25 mm corresponds approximately to 2 SDs above the average mean motion for the healthy older control group (mean = 0.10 mm, SD = 0.07), and/or at least 5 isolated movements of more than 0.5 mm from one brain volume as compared to the previous volume.

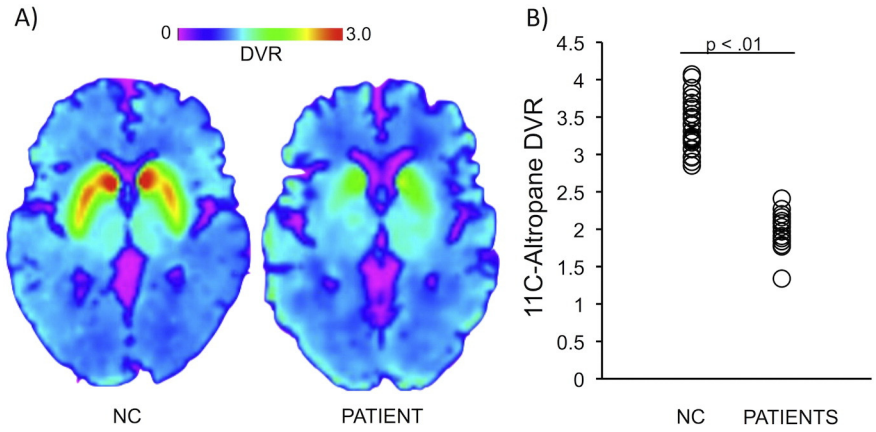


**Fig. 1.** A) An example image of 11-C Altropane binding is shown for a normal control and a patient with Parkinson's disease. The striatal ROI was identified as the 1000 voxels with peak radioactivity uptake. B) Striatal DAT availability (11C-Altropane DVR) is significantly lower in patients with nigrostriatal dopamine loss (dementia with Lewy bodies and Parkinson's disease) compared with age-matched normal control participants (NC).

For the remaining subjects, the 6 estimated motion parameters and other sources of variance unlikely to represent signal of neuronal origin (global signal, cerebrospinal fluid signal, deep cerebral white matter signal and the first temporal derivatives of these waveforms; Van Dijk et al., 2010) were removed by regression, saving the residual timecourses for each voxel for further analysis.

Bilateral caudate and putamen ROIs were defined based on the volumetric segmentation and co-registered to the fMRI data using boundary-based registration (Greve and Fischl, 2009) followed by registration to standard MNI152 space. In a first step, the putamen seed region was further separated into hemispheres and anterior and posterior putamen (cf Hacker et al., 2012 for details). However, connectivity from all four putamen subregions converged on a highly similar bilateral target in midbrain. Therefore, connectivity from the putamen to the midbrain target ROI was functionally defined based on average whole-brain correlation using the entire putamen. Peak coordinates of midbrain connectivity in the healthy controls were identified at (right/left) $x = 10/-8$, $y = -8/-10$, $z = -12/-12$ and a 6 mm sphere was added to capture individual variation around the peak. This ROI converges spatially with the substantia nigra ROI identified by Tomasi and Volkow (2014) ($x = \pm 12$, $y = -12$, $z = -12$).

We also found the putamen to be negatively correlated with the sensori-motor cortex and included these targets in the analysis. Control targets for which we did not expect an association with DAT availability in LBD were functionally defined targets on average whole-brain correlation maps of the caudate seed (thalamus and anterior cingulate cortex; di Martino et al., 2008; Hacker et al., 2012). All a-priori defined ROIs from the normal controls (Fig. 2) were then applied to the patient

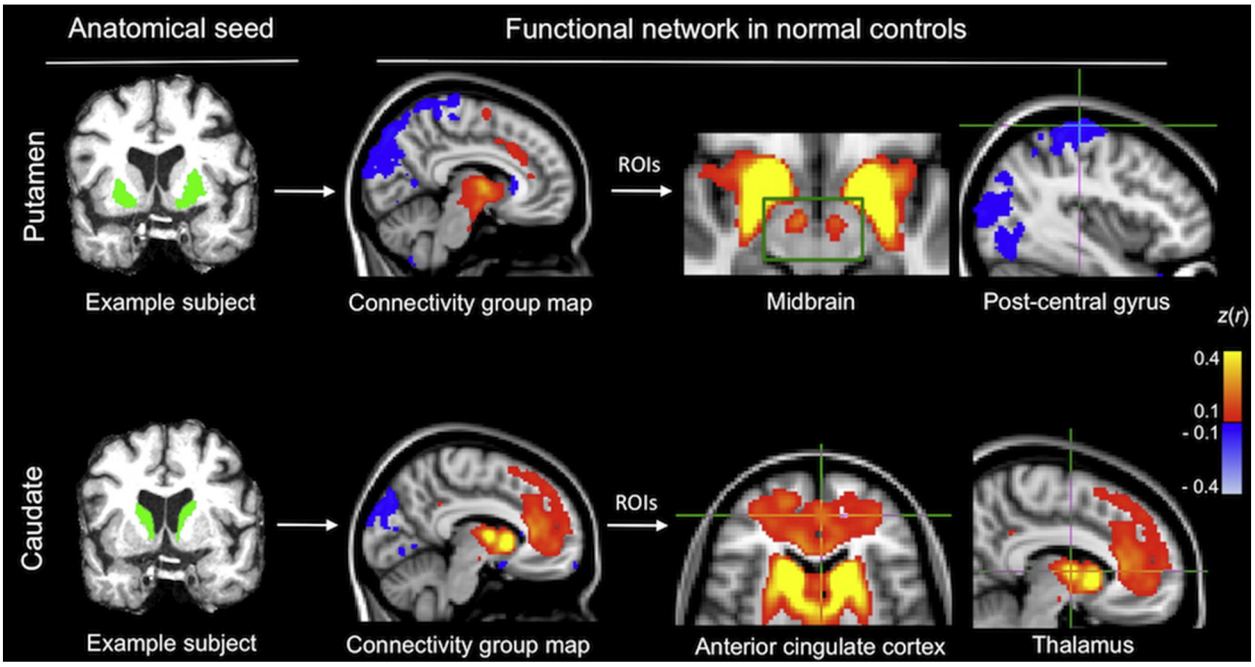


**Fig. 2.** Putamen and caudate seeds were defined based on anatomy from the individual subject structural MRI. Example putamen and caudate ROIs for one subject are shown. Whole-brain functional connectivity MRI maps using the putamen and caudate as seed region were then calculated in 29 clinically normal older adults to define regions of interest for further analyses in the patients. ROIs were identified as peak connectivity estimates of known regions within the caudate and putamen networks (Di Martino et al., 2008; Hacker et al., 2012). For the putamen network we selected peaks in the right and left midbrain (MNI coordinates right $x = 10$, $y = -8$, $z = -12$, left $x = -8$, $y = -10$, $z = -12$) and right and left postcentral gyrus (MNI coordinates right $x = 36$, $y = -26$, $z = 68$, left $x = -34$, $y = -20$, $z = 68$). For the caudate network we included peaks in the anterior cingulate cortex (MNI coordinates $x = -2$, $y = 46$, $z = 6$) and right and left anterior thalamus (MNI coordinates right $x = 10$, $y = -2$, $z = 6$, left $x = -10$, $y = -4$, $z = 8$).

group and for each patient the correlation between timeseries from (1) putamen and midbrain, (2) putamen and sensori-motor cortex (postcentral gyrus), (3) caudate and anterior cingulate, and (4) caudate and anterior thalamus were calculated. Since our main hypothesis was a positive association between midbrain–putamen functional connectivity and striatal DAT availability within this patient group, the main analysis consisted of Pearson's correlations and linear regression between fMRI functional connectivity and striatal PET DAT signal at a significance threshold of $p < 0.05$ (1-tailed). In an additional analysis we also explored the correlations between DAT availability and functional connectivity in the reference sample of healthy controls. These latter results should be interpreted cautiously, however, because these data are not independent from those used to define the seeds. Direct comparisons between patients and healthy controls were not computed because of differences in the fMRI acquisitions.

## 3. Results

Of chief interest, putamen–midbrain functional connectivity was associated with striatal DAT availability such that weaker connectivity was related to lower DAT signal ($r = 0.38$, $p = 0.05$, Fig. 3). Lower Altropane DVR was also associated with a less negative correlation between the putamen and the postcentral gyrus ($r = -0.37$, $p = 0.05$; Fig. 3). Striatal DAT availability was not related to functional connectivity between the caudate and the anterior cingulate cortex ($p = -0.22$, $p = 0.17$) or to functional connectivity between the caudate and the anterior thalamus ($r = -0.04$, $p = 0.86$). Controlling for mean head motion as a covariate in the analysis increased the correlation between DAT density and putamen–midbrain connectivity to $r = 0.44$ ($p = 0.03$).

Seven patients were excluded based on this additional quality control step. Although the identification of these subtle motion artifacts beyond the objective thresholds we set for movement parameters, is somewhat subjective, we find it important to demonstrate that for this sub-sample ($N = 13$), the correlations of striatal DAT density with putamen–midbrain connectivity ($r = 0.52$, $p = 0.04$) and putamen–postcentral gyrus ($r = -0.50$, $p = 0.04$) were still present. In a further set of control analyses, age, disease duration, subcortical atrophy, Hoehn and Yahr stage, and levodopa equivalent dose during the fMRI scan were explored in this subsample as possible confounding variables of the association between Altropane DVR and functional connectivity, beyond head motion. Notably, the association between functional connectivity MRI and DAT availability was reduced to trend-level when we accounted for medication (Table 1) as levodopa equivalent dose shared an association with both DAT availability ($r = -0.55$, $p = 0.03$) and putamen functional connectivity estimates (midbrain: $r = -0.54$, $p = 0.03$; postcentral gyrus: $r = 0.45$, $p = 0.06$). Importantly, however, no single covariate could fully explain the association between Altropane DVR and functional connectivity, indicating a direct association between measures of striatal dopamine functions and functional connectivity estimates beyond their shared association with disease severity.

**Table 1**
Linear regression of Altropane DVR on connectivity with covariates listed in parentheses.

| Outcome (fcMRI) | Predictors | Beta | p |
|---|---|---|---|
| Putamen−midbrain | Altropane DVR | 0.52 | 0.03 |
| | Altropane DVR(H & Y) | 0.50 | 0.07 |
| | Altropane DVR(Levodopa dose) | 0.32 | 0.17 |
| | Altropane DVR(Age) | 0.45 | 0.08 |
| | Altropane DVR(Subcortical atrophy) | 0.69 | 0.04 |
| Putamen−postcentral gyrus | Altropane DVR | −0.50 | 0.04 |
| | Altropane DVR(H & Y) | −0.33 | 0.16 |
| | Altropane DVR(Levodopa dose) | −0.36 | 0.14 |
| | Altropane DVR(Age) | −0.78 | <0.01 |
| | Altropane DVR(Subcortical atrophy) | −0.68 | 0.04 |

H & Y — Hoehn and Yahr clinical stage.

Incidentally, the associations between DAT density and putamen connectivity estimates were not present in the healthy controls (midbrain: $r = 0.16$, $p = 0.21$; post-central gyrus: $r = -0.01$, $p = 0.50$, co-varied for mean motion). Rather, in the healthy controls striatal DAT availability was significantly associated with connectivity between caudate and anterior thalamus ($r = 0.35$, $p = 0.04$, co-varied for mean motion) and, at trend-level, with the connectivity between caudate and anterior cingulate ($r = 0.24$, $p = 0.11$, co-varied for mean motion).

Patients with and without cognitive impairment did not differ significantly in any of the functional connectivity estimates (all p values > 0.05) and because of the limited sample size we were unable to assess additional or interacting effects of cognitive impairment in the current study. The patients with cognitive impairment are highlighted in green in the scatterplots.

## 4. Discussion

Previous research has shown reductions in functional connectivity between the midbrain and the putamen in group comparisons between healthy control subjects and patients with Parkinson's disease. Although functional connectivity MRI is a popular and reliable method for assessing the organization of functional networks in the brain, it remains challenging to relate inter-individual differences in connectivity strength between two regions to the integrity of the underlying neural pathways.

In the current study, we combined resting state fMRI and PET to show that individual differences in midbrain–putamen functional connectivity in patients with nigrostriatal dopamine loss are proportional

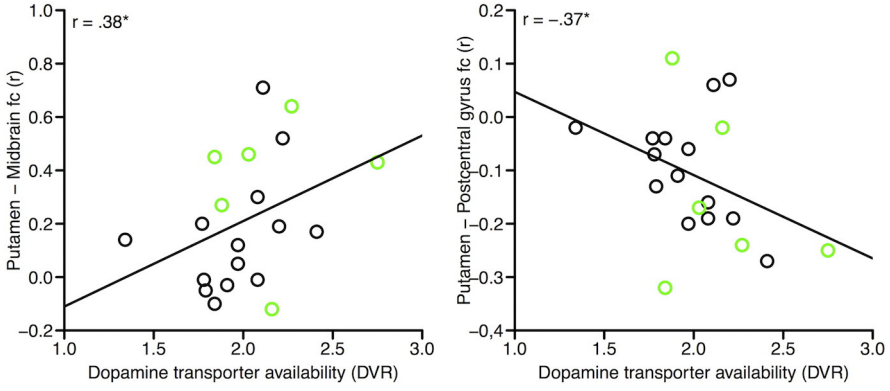


**Fig. 3.** Greater striatal DAT availability (Altropane DVR) is related to stronger connectivity of the putamen to midbrain and to increasingly negative correlation of the putamen to postcentral gyrus. * = p < .05. Patients with cognitive impairment are highlighted in green. For additional quality control, whole-brain functional connectivity maps were generated for the patients and inspected for remaining movement artifacts in the form of a ring activation pattern at the edges of the brain (a commonly mentioned residual effect of motion on fMRI data; cf Beckmann et al., 2000; Satterthwaite et al., 2013; White et al., 2014).

to measures of integrity of the dopamine system. DAT availability in these patients was unrelated to connectivity within the caudate–thalamic–prefrontal loop. Histopathology studies have shown specific losses of dopaminergic nigro-striatal projections in Parkinson's disease and dementia with Lewy bodies that are dissociable from normal aging (Fearnley and Lees, 1991) and our findings suggest that putamen functional connectivity estimates are sensitive to impairment of this projection. Pertaining to this point, we found no evidence for an association between putamen–midbrain connectivity and DAT availability in the healthy controls. This interpretation does not preclude the possibility that caudate networks may also play a role in disease progression and relate to the cognitive impairment that develops in a subset of patients. Here, we were unable to disentangle differential patterns of striatal connectivity in patients with and without dementia because of the small number of cognitively impaired subjects.

Studies applying a levodopa challenge in young adults (Kelly et al., 2009; Cole et al., 2013) and patients with Parkinson's disease (Jech et al., 2013) have shown acute increases in midbrain functional connectivity following drug administration. Taken together, our results and the results from pharmacological fMRI studies show that midbrain functional connectivity can be sensitive to the overall trait of the dopamine system (i.e. striatal DAT availability) as well to as short-term changes in dopamine state (i.e. following pharmacological intervention). In line with this, while levodopa dose accounted for a part of the association between DAT availability and putamen connectivity, levodopa dose did not fully explain the resting-state functional connectivity estimates attributable to DAT availability. That said, further research is needed to validate the usefulness of functional connectivity as a correlate of PET-based imaging of the dopamine system also in patients off medication and in very early stages of the disease. In the current study, patients were in a moderate disease stage and tested on medication to avoid movement in the scanner and to reduce patient burden. With respect to accurately disentangling the effects of levodopa dose and DAT availability on functional connectivity, the fact that all patients were tested on medication is a potential limitation of the current study.

In addition to midbrain–putamen connectivity, we found that DAT availability was related to negative correlations between putamen signal and the postcentral gyrus. Negative correlations are often seen in resting-state studies of the striatum (e.g. di Martino et al., 2008), and appear to be less negative in Parkinson's disease (Göttlich et al., 2013; Hacker et al., 2012; Wu et al., 2009; Yu et al., 2013), suggesting that putamen correlations of either sign tend towards zero as striatal dopamine terminals are lost and the disease progresses (Olde Dubbelink et al., 2014). Our results confirm that weaker estimates of either sign are related to the disease process. However, it should be noted that negative correlations are difficult to interpret in functional connectivity analyses (Weissenbacher et al., 2009), and it is unclear whether negative correlations between putamen and postcentral gyrus reflect the integrity of anatomical projections. As Lewy bodies tend to spare the sensori-motor cortices until late in the disease (Braak et al., 2004), negative correlations between the putamen and sensori-motor areas may relate to the neurodegenerative disease process through downstream effects of nigrostriatal dopaminergic depletion. Of note, a whole-brain explorative correlational analysis by Baik et al. (2014) suggested that associations between DAT availability and striatal connectivity may also exist for regions outside of putamen–thalamic–cortical networks, which we did not assess here.

One limitation of the current study may be that our measure of striatal DAT availability does not distinguish between caudate and putamen or between brain hemispheres. We chose this approach because it ensures that DVR estimation was fully automated and would not be affected by differences in striatal volume between participants or by errors in registration, which can be substantial in patient groups (e.g. Reig et al., 2007). Our striatal estimate of DAT availability accurately distinguished between patients and normal controls, and measures of DAT availability correlated with measures of symptom severity as expected.

A further limitation of this study is the small sample size, which was due to a priori screening of patients for head motion during fMRI scanning. Motion is a common problem in fMRI studies of patients with movement disorders (Hacker et al., 2012), and we opted for analytic rigor over larger numbers of subjects. We hope that with public databases becoming increasingly available, it will in the future be possible to replicate our results in a larger independent sample.

In conclusion, this study shows that functional connectivity between the midbrain and the striatum is linked to the integrity of the dopamine system in patients with Lewy body diseases. These findings suggest that midbrain–striatum functional connectivity may provide a useful indicator of underlying pathology in diseases characterized by nigrostriatal dopamine loss.

## Acknowledgements

Data from cognitively normal older adults were collected in collaboration with contributors to the Harvard Aging Brain Study (http://www.martinos.org/harvardagingbrain/Acknowledgements.html); in particular we thank Randy Buckner, Trey Hedden and Reisa Sperling for providing the research funding and data for the healthy control group. The Massachusetts General Hospital Molecular Imaging PET Core provided assistance with PET Imaging. We thank Alex Becker, Marta Marquie, and Aaron Schultz for assistance with data analysis. This research was supported by The Michael J. Fox Foundation (to SNG and JHG), National Alzheimer's Coordinating Center Collaborative Project 5 U01 AG016976-11 (to SNG, KAJ, and JHG), the National Institute of Neurological Disorders and Stroke R21NS090243-01 (to SNG, JHG, and KAJ), the National Institute on Aging P50 AG005134-32, (to JHG), National Institute of Neurological Disorders and Stroke (to KAJ), the National Institute on Aging (to KAJ), the Alzheimer's Disease Association (to KAJ), and the Harvard Center for Neurodegeneration and Repair Pilot grant (to SNG). AR was supported by a Marie Curie International Outgoing Fellowship from the European Commission. This research was carried out in whole or in part at the Athinoula A. Martinos Center for Biomedical Imaging at the Massachusetts General Hospital, using resources provided by the Center for Functional Neuroimaging Technologies, P41EB015896, a P41 Biotechnology Resource Grant supported by the National Institute of Biomedical Imaging and Bioengineering, National Institutes of Health. This work also involved the use of instrumentation supported by the National Institutes of Health Shared Instrumentation Grant Program and/or High-End Instrumentation Grant Program (grant numbers S10RR023401, S10RR019307, S10RR019254, S10RR023043). The authors declare no competing financial interests.

## References

Baik, K., Cha, J., Ham, J.H., Baek, G.-M., Sunwoo, M.K., Hong, J.Y., Shin, N.-Y., Kim, J.S., Lee, J.-M., Lee, S.-K., Sohn, Y.H., Lee, P.H., 2014. Dopaminergic modulation of resting-state functional connectivity in de novo patients with Parkinson's disease. Hum. Brain Mapp. 35 (11), 5431–5441. http://dx.doi.org/10.1002/hbm.2256124938993.

Beckmann, C.F., Noble, J.A., Smith, S.M., 2000. Artefact detection in FMRI data using independent component analysis. Neuroimage 11 (5), S614–S615. http://dx.doi.org/10.1016/S1053-8119(00)91544-1.

Braak, H., Ghebremedhin, E., Rüb, U., Bratzke, H., Del Tredici, K., 2004. Stages in the development of Parkinson's disease-related pathology. Cell Tissue Res. 318 (1), 121–134. http://dx.doi.org/10.1007/s00441-004-0956-915338272.

Brooks, D.J., Pavese, N., 2011. Imaging biomarkers in Parkinson's disease. Prog. Neurobiol. 95 (4), 614–628. http://dx.doi.org/10.1016/j.pneurobio.2011.08.00921896306.

Buckner, R.L., Head, D., Parker, J., Fotenos, A.F., Marcus, D., Morris, J.C., Snyder, A.Z., 2004. A unified approach for morphometric and functional data analysis in young, old, and demented adults using automated atlas-based head size normalization: reliability and validation against manual measurements of total intracranial volume. Neuroimage 23 (2), 724–738. http://dx.doi.org/10.1016/j.neuroimage.2004.06.018.

Cole, D.M., Oei, N.Y.L., Soeter, R.P., Both, S., van Gerven, J.M.A., Rombouts, S.A.R.B., Beckmann, C.F., 2013. Dopamine-dependent architecture of cortico-subcortical network connectivity. Cereb. Cortex 23 (7), 1509–1516. http://dx.doi.org/10.1093/cercor/bhs13622645252.

Colloby, S.J., McParland, S., O'Brien, J.T., Attems, J., 2012. Neuropathological correlates of dopaminergic imaging in Alzheimer's disease and Lewy body dementias. Brain 135 (9), 2798–2808. http://dx.doi.org/10.1093/brain/aws21122961551.

Di Martino, A., Scheres, A., Margulies, D.S., Kelly, A.M.C., Uddin, L.Q., Shehzad, Z., Biswal, B., Walters, J.R., Castellanos, F.X., Milham, M.P., 2008. Functional connectivity of human striatum: a resting state FMRI study. Cereb. Cortex 18 (12), 2735–2747. http://dx.doi.org/10.1093/cercor/bhn04118400794.

Emre, M., Aarsland, D., Brown, R., Burn, D.J., Duyckaerts, C., Mizuno, Y., Broe, G.A., Cummings, J., Dickson, D.W., Gauthier, S., Goldman, J., Goetz, C., Korczyn, A., Lees, A., Levy, R., Litvan, I., McKeith, I., Olanow, W., Poewe, W., Quinn, N., Sampaio, C., Tolosa, E., Dubois, B., 2007. Clinical diagnostic criteria for dementia associated with Parkinson's disease. Mov. Disord. 22 (12), 1689–1707. http://dx.doi.org/10.1002/mds.2150717542011.

Fearnley, J.M., Lees, A.J., 1991. Ageing and Parkinson's disease: substantia nigra regional selectivity. Brain 114 (5), 2283–2301. http://dx.doi.org/10.1093/brain/114.5.22831933245.

Fischl, B., Salat, D.H., Busa, E., Albert, M., Dieterich, M., Haselgrove, C., van der Kouwe, A., Killiany, R., Kennedy, D., Klaveness, S., Montillo, A., Makris, N., Rosen, B., Dale, A.M., 2002. Whole brain segmentation: automated labeling of neuroanatomical structures in the human brain. Neuron 33 (3), 341–355. http://dx.doi.org/10.1016/S0896-6273(02)00569-X11832223.

Fischman, A.J., Bonab, A.A., Babich, J.W., Livni, E., Alpert, N.M., Meltzer, P.C., Madras, B.K., 2001. [(11)C, (127)I] Altropane: a highly selective ligand for PET imaging of dopamine transporter sites. Synapse 39 (4), 332–342. http://dx.doi.org/10.1002/1098-2396(20010315)39:4<332::AID-SYN1017>3.0.CO;2-X11169784.

Göttlich, M., Münte, T.F., Heldmann, M., Kasten, M., Hagenah, J., Krämer, U.M., 2013. Altered resting state brain networks in Parkinson's disease. PLOS One 8 (10), e77336. http://dx.doi.org/10.1371/journal.pone.007733624204812.

Greve, D.N., Fischl, B., 2009. Accurate and robust brain image alignment using boundary-based registration. Neuroimage 48 (1), 63–72. http://dx.doi.org/10.1016/j.neuroimage.2009.06.06019573611.

Hacker, C.D., Perlmutter, J.S., Criswell, S.R., Ances, B.M., Snyder, A.Z., 2012. Resting state functional connectivity of the striatum in Parkinson's disease. Brain 135 (12), 3699–3711. http://dx.doi.org/10.1093/brain/aws28123195207.

Hadley, J.A., Nenert, R., Kraguljac, N.V., Bolding, M.S., White, D.M., Skidmore, F.M., Visscher, K.M., Lahti, A.C., 2014. Ventral tegmental area/midbrain functional connectivity and response to antipsychotic medication in schizophrenia. Neuropsychopharmacology 39 (4), 1020–1030. http://dx.doi.org/10.1038/npp.2013.30524165885.

Hughes, A.J., Daniel, S.E., Kilford, L., Lees, A.J., 1992. Accuracy of clinical diagnosis of idiopathic Parkinson's disease: a clinico-pathological study of 100 cases. J. Neurol. Neurosurg. Psychiatry 55 (3), 181–184. http://dx.doi.org/10.1136/jnnp.55.3.181.

Innis, R.B., Seibyl, J.P., Scanley, B.E., Laruelle, M., Abi-Dargham, A., Wallace, E., Baldwin, R.M., Zea-Ponce, Y., Zoghbi, S., Wang, S., 1993. Single photon emission computed tomographic imaging demonstrates loss of striatal dopamine transporters in Parkinson disease. Proc. Natl. Acad. Sci. U. S. A. 90 (24), 11965–11969. http://dx.doi.org/10.1073/pnas.90.24.119658265656.

Jech, R., Mueller, K., Schroeter, M.L., Růžička, E., 2013. Levodopa increases functional connectivity in the cerebellum and brainstem in Parkinson's disease. Brain 136 (7), e234. http://dx.doi.org/10.1093/brain/awt01523370091.

Jenkinson, M., Bannister, P., Brady, M., Smith, S.M., 2002. Improved optimization for the robust and accurate linear registration and motion correction of brain images. NeuroImage 17 (2), 825–841. http://dx.doi.org/10.1006/nimg.2002.113212377157.

Kelly, C., de Zubicaray, G., Di Martino, A., Copland, D.A., Reiss, P.T., Klein, D.F., Castellanos, F.X., Milham, M.P., McMahon, K., 2009. L-dopa modulates functional connectivity in striatal cognitive and motor networks: a double-blind placebo-controlled study. J. Neurosci. 29 (22), 7364–7378. http://dx.doi.org/10.1523/JNEUROSCI.0810-09.200919494158.

Laruelle, M., Abi-Dargham, A., van Dyck, C.H., Gil, R., D'Souza, C.D., Erdos, J., McCance, E., Rosenblatt, W., Fingado, C., Zoghbi, S.S., Baldwin, R.M., Seibyl, J.P., Krystal, J.H., Charney, D.S., Innis, R.B., 1996. Single photon emission computerized tomography imaging of amphetamine-induced dopamine release in drug-free schizophrenic subjects. Proc. Natl. Acad. Sci. U. S. A. 93 (17), 9235–9240. http://dx.doi.org/10.1073/pnas.93.17.92358799184.

Logan, J., Fowler, J.S., Volkow, N.D., Wolf, A.P., Dewey, S.L., Schlyer, D.J., MacGregor, R.R., Hitzemann, R., Bendriem, B., Gatley, S.J., 1990. Graphical analysis of reversible radioligand binding from time-activity measurements applied to [N–11C-methyl]-(-)-cocaine PET studies in human subjects. J. Cereb. Blood Flow Metab. 10 (5), 740–747. http://dx.doi.org/10.1038/jcbfm.1990.1272384545.

Marquie, M., Locascio, J.J., Rentz, D.M., Becker, J., Hedden, T., Johnson, K.A., Growdon, J.H., Gomperts, S.N., 2014. Striatal and extrastriatal dopamine transporter levels relate to cognition in Lewy body diseases: an 11C altropane positron emission tomography study. Alz. Res. Therapy 6 (5–8), 52. http://dx.doi.org/10.1186/s13195-014-0052-7.

McKeith, I.G., et al., 2005. Diagnosis and management of dementia with Lewy bodies: third report of the DLB Consortium. Neurol. 65 (12), 1863–1872. http://dx.doi.org/10.1212/01.wnl.0000187889.17253.b116237129.

Meltzer, C.C., Leal, J.P., Mayberg, H.S., Wagner, H.N., Frost, J.J., 1990. Correction of PET data for partial volume effects in human cerebral cortex by MR imaging. J. Comput. Assist. Tomogr. 14 (4), 561–570. http://dx.doi.org/10.1097/00004728-199007000-000112370355.

O'Brien, J.T., Colloby, S., Fenwick, J., Williams, E.D., Firbank, M., Burn, D., Aarsland, D., McKeith, I.G., 2004. Dopamine transporter loss visualized with FP-CIT SPECT in the differential diagnosis of dementia with Lewy bodies. Arch. Neurol. 61 (6), 919–925. http://dx.doi.org/10.1001/archneur.61.6.91915210531.

Olde Dubbelink, K.T., Schoonheim, M.M., Deijen, J.B., Twisk, J.W., Barkhof, F., Berendse, H.W., 2014. Functional connectivity and cognitive decline over 3 years in Parkinson disease. Neurology 83 (22), 2046–2053. http://dx.doi.org/10.1212/WNL.0000000000000102025355821.

Quarantelli, M., Berkouk, K., Prinster, A., Landeau, B., Svarer, C., Balkay, L., Alfano, B., Brunetti, A., Baron, J.C., Salvatore, M., 2004. Integrated software for the analysis of brain PET/SPECT studies with partial-volume-effect correction. J. Nucl. Med. 45 (2), 192–20114960635.

Reig, S., Penedo, M., Gispert, J.D., Pascau, J., Sánchez-González, J., García-Barreno, P., Desco, M., 2007. Impact of ventricular enlargement on the measurement of metabolic activity in spatially normalized PET. Neuroimage 35 (2), 748–758. http://dx.doi.org/10.1016/j.neuroimage.2006.12.01517275338.

Ryan, J.J., Paolo, A.M., 1992. A screening procedure for estimating premorbid intelligence in the elderly. Clin. Neuropsychol. 6 (1), 53–62. http://dx.doi.org/10.1080/13854049208404117.

Satterthwaite, T.D., Elliott, M.A., Gerraty, R.T., Ruparel, K., Loughead, J., Calkins, M.E., Eickhoff, S.B., Hakonarson, H., Gur, R.C., Gur, R.E., Wolf, D.H., 2013. An improved framework for confound regression and filtering for control of motion artifact in the preprocessing of resting-state functional connectivity data. Neuroimage 64, 240–256. http://dx.doi.org/10.1016/j.neuroimage.2012.08.05222926292.

Schultz, A.P., Chhatwal, J.P., Huijbers, W., Hedden, T., Van Dijk, K.R., McLaren, D.G., Ward, A.M., Wigman, S., Sperling, R.A., 2014. Template based ortation: a method for functional connectivity analysis with a priori templates. NeuroImage 15, 620–636.

Shaw, E.E., Schultz, A.P., Sperling, R., Hedden, T., 2015. Functional connectivity in multiple cortical networks is associated with performance across cognitive domains in older adults. Brain Connectivity epub ahead of print.

Spencer, T.J., Biederman, J., Faraone, S.V., Madras, B.K., Bonab, A.A., Dougherty, D.D., Batchelder, H., Clarke, A., Fischman, A.J., 2013. Functional genomics of attention-deficit/hyperactivity disorder (ADHD) risk alleles on dopamine transporter binding in ADHD and healthy control subjects. Biol. Psychiatry 74 (2), 84–89. http://dx.doi.org/10.1016/j.biopsych.2012.11.01023273726.

Tomasi, D., Volkow, N.D., 2014. Functional connectivity of substantia nigra and ventral tegmental area: maturation during adolescence and effects of ADHD. Cereb. Cortex 24 (4), 935–944. http://dx.doi.org/10.1093/cercor/bhs38223242198.

Tomlinson, C.L., Stowe, R., Patel, S., Rick, C., Gray, R., Clarke, C.E., 2010. Systematic review of levodopa dose equivalency reporting in Parkinson's disease. Mov. Disord. 25 (15), 2649–2653. http://dx.doi.org/10.1002/mds.2342921069833.

Van Dijk, K.R.A., Hedden, T., Venkataraman, A., Evans, K.C., Lazar, S.W., Buckner, R.L., 2010. Intrinsic functional connectivity as a tool for human connectomics: theory, properties, and optimization. J. Neurophysiol. 103 (1), 297–321. http://dx.doi.org/10.1152/jn.00783.200919889849.

Van Dijk, K.R.A., Sabuncu, M.R., Buckner, R.L., 2012. The influence of head motion on intrinsic functional connectivity MRI. NeuroImage 59 (1), 431–438. http://dx.doi.org/10.1016/j.neuroimage.2011.07.04421810475.

Weissenbacher, A., Kasess, C., Gerstl, F., Lanzenberger, R., Moser, E., Windischberger, C., 2009. Correlations and anticorrelations in resting-state functional connectivity MRI: A quantitative comparison of preprocessing strategies. NeuroImage 47 (4), 1408–1416. http://dx.doi.org/10.1016/j.neuroimage.2009.05.00519442749.

White, T., Muetzel, R., Schmidt, M., Langeslag, S.J., Jaddoe, V., Hofman, A., Calhoun, V.D., Verhulst, F.C., Tiemeier, H., 2014. Time of acquisition and network stability in pediatric resting-state functional magnetic resonance imaging. brain. Connection 6, 417–427.

Wu, T., Wang, J., Wang, C., Hallett, M., Zang, Y., Wu, X., Chan, P., 2012. Basal ganglia circuits changes in Parkinson's disease patients. Neurosci. Lett. 524 (1), 55–59. http://dx.doi.org/10.1016/j.neulet.2012.07.01222813979.

Wu, T., Wang, L., Chen, Y., Zhao, C., Li, K., Chan, P., 2009. Changes of functional connectivity of the motor network in the resting state in Parkinson's disease. Neurosci. Lett. 460 (1), 6–10. http://dx.doi.org/10.1016/j.neulet.2009.05.04619463891.

Yu, R., Liu, B., Wang, L., Chen, J., Liu, X., 2013. Enhanced functional connectivity between putamen and supplementary motor area in Parkinson's disease patients. PLOS One 8 (3), e59717. http://dx.doi.org/10.1371/journal.pone.005971723555758.